In Vitro Model for Transport of Solutes in Three-Phase System I: Theoretical Principles

RANDALL G. STEHLE* and WILLIAM I. HIGUCHI▲

Abstract □ A diffusional model describing steady-state transport of neutral compounds and ionizing weak acids and bases in the three-phase (water–oil–water) system is presented. The present study applies this model, consisting of three barriers in series, to a theoretical and experimental exploration of the pH–partition theory of drug absorption. The model correlates transport rates with primary factors (pH and partition coefficient) as well as with buffer strength, diffusion coefficients, and the rate of agitation in the aqueous phases. For strictly neutral solutes, any one barrier may become rate limiting. When solute partition coefficients become sufficiently large, the transport rates level off to a maximal value. For weak acids and bases, the relative rates generally follow titration curves. Under certain pH conditions, maximal rates of ionizing electrolytes may be double that of the neutral solute. In all cases, a maximal rate with respect to an increasing partition coefficient is predicted. Experimental data in previous studies were analyzed, evaluating relative contributions to the total barrier by the lipid and aqueous phases.

Keyphrases □ Transport of solutes—three-phase (w/o/w) system, theoretical considerations □ Solute transport—three-phase (w/o/w) system, theoretical considerations □ Three-phase (water–oil–water) system—solute transport, theoretical considerations □ Diffusional model—solute transport in three-phase (w/o/w) system, relationship to pH–partition theory □ pH–partition theory—effect of transport rates in three-phase (w/o/w) system □ Absorption, drug—three-phase (w/o/w) model proposed to study pH–partition theory

The literature has been populated in recent years by many papers concerning drug absorption. This is justifiably so; such studies lead to the better understanding of what occurs between the time that a drug is orally administered and the time that it reaches the site of action. The vast majority of this work has tried to elucidate the basic mechanisms operant in the *in vivo* transport of solutes. Inherent in these studies is the assertion that most drugs are absorbed by passive transfer or simple diffusion; the substance crosses the absorption barrier at a rate proportional to its chemical or electrochemical gradient across the barrier. The physical nature of the membrane determines what types, configurations, and sizes of solutes may cross it.

The basic problem with most approaches, however, has been the lack of a model comprehensive enough to allow inclusion of, and interrelation among, various physicochemical factors present in the three-phase system and prediction of the effect of these factors on the rate of solute movement through the system. Such factors include the dimensions of the system and its individual phases, buffer strength, ionic strength, and chemical equilibria between species. Thus, after the undeniably classic pH–partition thesis of drug absorption was formulated in the late 1950's (1–5), many researchers were able to demonstrate the effects of pH and the oil–water partition coefficient on absorption of solutes. Results of different *in vivo* and even idealized *in vitro* studies could not be meaningfully compared or interpreted, however, especially in cases where anomalous behavior occurred; this was primarily due to the lack of accurate definition of the experimental systems.

At the very least, an idealized model of the barrier to absorption should include an effective, predominantly aqueous barrier in series with the lipoidal membrane barrier. Hydrodynamics predict the existence of such a barrier near a surface. Moreover, the presence of largely hydrophilic mucoproteins at the intestinal mucosal interface (adsorbed and/or integral with the lipid barrier) should enhance the magnitude of this aqueous barrier. A more rigorous model of the membrane would treat it as a heterogeneous phase rather than a lipoidal "slab."

The purpose of the present work is to present a comprehensive, somewhat idealized, and well-defined *in vitro* model describing movement of solutes in the three-phase system. The model, with its framework of interrelated physicochemical variables, incorporates significant mechanistic concepts which may hopefully serve as a baseline for interpreting the far more complex biological situation.

LITERATURE

Various mathematical approaches have been utilized in the modelistic representation of drug transport. There are the nonsteady-state, first-order kinetic studies (6, 7), which follow concentrations of solute in each of three (apparently well-stirred) phases with time. The relationship between real physicochemical variables and the derived first-order transfer constants is not always apparent (8).

The two-phase (aqueous–lipid) model of Howard *et al.* (9, 10) for nonionizing solutes introduced the diffusional approach to the problem, postulating diffusional barriers and relating transport behavior to such factors as partition coefficient, diffusion barrier thickness, and diffusion coefficient. The concept was subsequently extended by Suzuki *et al.* (11, 12) to include ionizing solutes, bringing in the effect of pH.

Passow (13) developed a mathematical diffusional model for transport of substances in the renal tubule, taking into account the nonplanar geometry of the tubular surface and considering the cellular components themselves. His study did evaluate possible contributions by the aqueous diffusion barrier adjacent to the membrane.

THEORETICAL

The simplest model pertains to neutral, nonionizing substances. The model applicable to these compounds, R, appears in Fig. 1. Appearing on either side of the lipoidal barrier are aqueous diffusion barriers. Steady-state gradients are linear as shown, there being no interactions or equilibria with other species in the system and no dependence of diffusion coefficients on concentration.

In general, Fick's law applies at any location:

$$D_R \frac{\partial^2 R(x,t)}{\partial x^2} = \frac{\partial R(x,t)}{\partial t} \qquad \text{(Eq. 1)}$$

In the steady-state case, it is assumed that concentrations have no

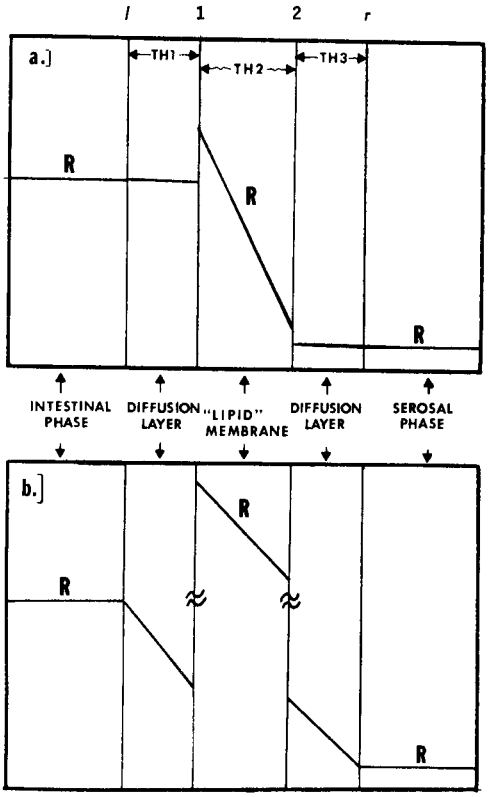

Figure 1—*Three-phase open model showing schematic concentration gradients in steady-state transport of neutral solutes, where: (a) R has low partition coefficient, and (b) R has high partition coefficient.*

time dependence. Therefore:

$$D_R \frac{d^2R(x)}{dx^2} = \frac{dR(x)}{dt} = 0 \qquad \text{(Eq. 2)}$$

in any barrier; hence, the transport rate, G (mass cm.$^{-2}$ sec.$^{-1}$), may be obtained by integration:

$$G = -D_R \frac{dR}{dx} = \text{constant} \qquad \text{(Eq. 3)}$$

Assumption of an open system allows maintenance of constant concentrations in the bulk aqueous phases. D_W, the aqueous diffusion coefficient of R, is assumed equal in both aqueous phases. KLH, R's oil–water partition coefficient, is considered the same at both interfaces, so:

$$KLH = \frac{C_1\,(\text{oil})}{C_1\,(\text{water})} = \frac{C_2\,(\text{oil})}{C_2\,(\text{water})} \qquad \text{(Eq. 4)}$$

where the subscripts 1 and 2 indicate left and right aqueous interfacial locations, respectively, as shown in Fig. 1.

The steady-state transport in this system may be summarized by a group of equations describing flux through each of the three barriers:

$$G_1 = D_W(R_l - R_1)/TH1 \qquad \text{(Eq. 5)}$$

$$G_2 = D_L(KLH)(R_1 - R_2)/TH2 \qquad \text{(Eq. 6)}$$

$$G_3 = D_W(R_2 - R_r)/TH3 \qquad \text{(Eq. 7)}$$

l and r refer to borders of the left and right bulk aqueous phases, respectively; D_W and D_L (cm.^{2} sec.$^{-1}$) are the aqueous and lipid diffusion coefficients of R, respectively; TH1 and TH3 are the effective[1] thicknesses of the "mucosal" and "serosal" diffusion layers (cm.), respectively; and TH2 is the membrane thickness. Concentrations are given in mmoles cm.$^{-3}$ or M.

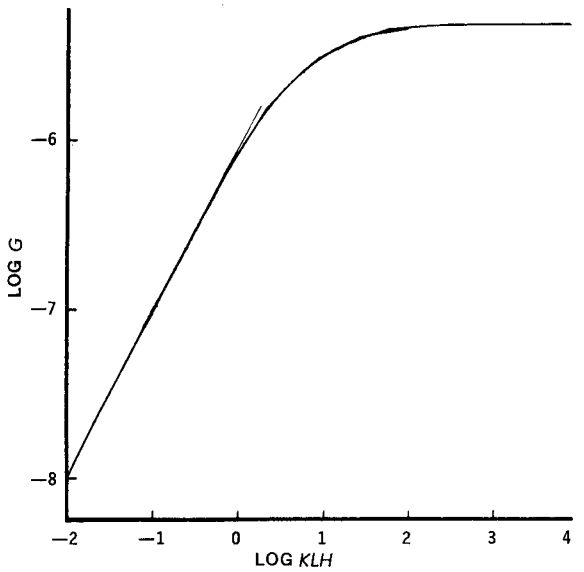

Figure 2—*Results of calculations for neutral solutes according to Eq. 8. All diffusion coefficients = 10^{-5} cm.^{2} sec.$^{-1}$. TH1 = TH3 = 100 μ; TH2 = 10^{-1} cm. ΔC = 10^{-2} M.*

At steady state, from Eq. 3, $G_1 = G_2 = G_3$, and one has the simple series barrier situation. Equations 5–7 give, as a solution:

$$G = (R_l - R_r)\Big/\left(\frac{TH1 + TH3}{D_W} + \frac{TH2}{(KLH)(D_L)}\right) \qquad \text{(Eq. 8)}$$

The transport rate is directly proportional to the overall concentration difference of the solute across the system. More significantly, it appears that G is directly proportional to the partition coefficient (as implied by the pH–partition theory) only as long as KLH is small enough to make the second term in the denominator much larger than the first term. Thus:

$$G = \frac{(KLH)(D_L)(R_l - R_r)}{TH2} \qquad \text{(Eq. 9)}$$

At larger values of KLH, depending on the relative values of TH1, TH2, TH3, D_W, and D_L, G loses its linear dependence on the partition coefficient and levels off to a maximal value. The second denominatorial term has now become negligible in comparison to the first. At low KLH values, the membrane is the entire barrier (Fig. 1*a*). At high values of KLH (Fig. 1*b*), the membrane is "shorted out"; G is limited by the aqueous diffusional barriers in series with the membrane.

Figure 2 illustrates results obtained for a typical solute–membrane system. Here, P, the permeability coefficient, defined as:

$$P = (D_L)(KLH)/TH2 \qquad \text{(Eq. 10)}$$

is equal to $10^{-4} \cdot KLH$. This implies an effective membrane thickness significantly greater than the 100 Å value usually associated with single membrane barriers and/or a low diffusion coefficient in the lipid phase. In Fig. 2, G rises linearly with KLH at low values of the latter but levels off to a maximum value ($C_l - C_r$ being constant).

Weak Bases—Figure 3 qualitatively illustrates the steady-state model for the transport of a weak base, RN, protonated at lower pH values to RNH^+; H2C/HC^- and BH/B^- represent buffers present in the serosal and mucosal phases, respectively. Only the uncharged form, RN, of the solute may penetrate the lipid phase[2]. Due to the existence of simultaneous transport and chemical equilibria in the system, curved concentration profiles may exist under cer-

[1] The contribution of convection to the overall transport process is assumed to be negligible (25).

[2] Therefore, the phenomenon of bulk flow through the membrane is assumed not to occur.

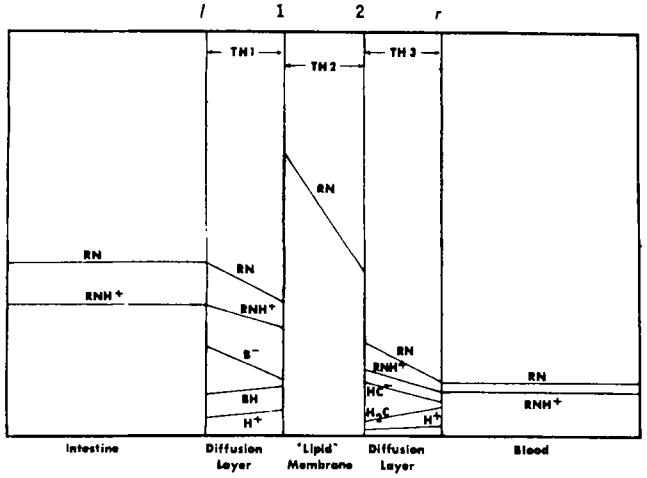

Figure 3—*Three-phase model showing schematic concentration profiles present in steady-state transport of weakly basic drugs, RN. RNH^+ is the protonated base; BH and B^- are forms of buffer in intestinal fluids; H^+ is hydrogen ion; H2C and HC^- are forms of the plasma buffer; and TH1, TH2, and TH3 are diffusion barrier thicknesses in the three phases and will keep their present definitions in subsequent discussions.*

tain conditions in Fig. 3.

The following equations describe the base model under steady-state conditions:

$$G_{II} = (KLH)(D_{L,RN})(RN_l - RN_2)/TH2 \quad \text{(Eq. 11)}$$

$$(TH1)(G_I) = D_{W,RNH^+}(RNH_l^+ - RNH_1^+) + D_{W,RN}(RN_l - RN_1) \quad \text{(Eq. 12)}$$

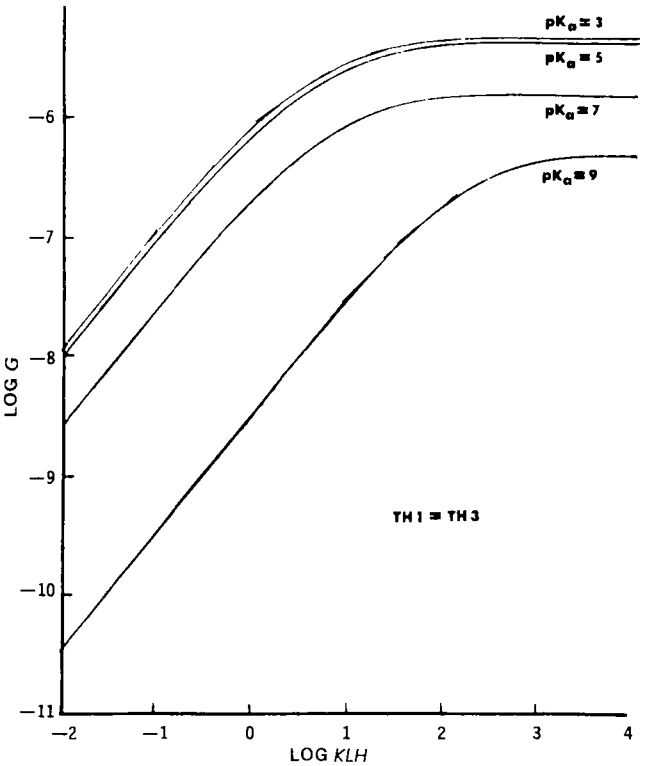

Figure 4—*Results of computer calculations for the steady-state model for the transport of basic drugs of various pKa's. G, the transport rate, is in mmoles cm.$^{-2}$ sec.$^{-1}$. Intestinal pH = 6.5; serosal pH = 7.4. Total intestinal buffer concentration ($HB + B^-$) = 10^{-2} M; total serosal buffer = 0.026 M, ΔC for drug = 10^{-2} M. TH1 = TH3 = 10^{-2} cm.; TH2 = 10^{-1} cm. K (intestinal buffer) = 10^{-6}; K (serosal buffer) = 6×10^{-7}.*

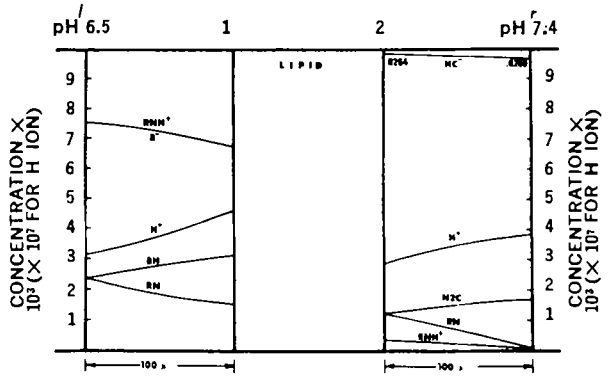

Figure 5—*Actual concentration profiles based on solution of Eqs. 11–17 in modified form and data from Fig. 4, along with computer-generated concentrations of the various species at the interfaces. The partition coefficient of the base = 100; pKa of base = 7; pKa of mucosal buffer = 6; K_a of serosal buffer = 6×10^{-7}. Boundary conditions include: G = 1.69×10^{-6} mmole cm.$^{-2}$ sec.$^{-1}$, $H_2^+ = 2.98 \times 10^{-8}$, $H_1^+ = 4.64 \times 10^{-7}$, $RN_2 = 1.30 \times 10^{-3}$, and $RN_1 = 1.47 \times 10^{-3}$.*

$$D_{W,B^-}(B_l^- - B_1^-) = D_{W,BH}(BH_l - BH_1) \quad \text{(Eq. 13)}$$

$$D_{W,RNH^+}(RNH_l^+ - RNH_1^+) = D_{W,H^+}(H_l^+ - H_1^+) + D_{W,BH}(BH_1 - BH_l) \quad \text{(Eq. 14)}$$

$$(TH3)(G_{III}) = D_{W,RN}(RN_2 - RN_r) + D_{W,RNH^+}(RNH_2^+ - RNH_r^+) \quad \text{(Eq. 15)}$$

$$D_{W,H2C}(H2C_r - H2C_2) = D_{W,HC^-}(HC_2^- - HC_r^-) \quad \text{(Eq. 16)}$$

$$D_{W,H^+}(H_r^+ - H_2^+) + D_{W,H2C}(H2C_r - H2C_2) = D_{W,RNH^+}(RNH_2^+ - RNH_r^+) \quad \text{(Eq. 17)}$$

H^+ in these equations is hydrogen ion. Subscripts on diffusion coefficients refer to individual species, and other symbols are as previously defined. Equation 11 describes the movement of RN through the lipid membrane. Equations 12 and 15 give the total solute transport in the left and right aqueous barriers, respectively. Equations 13 and 16 are the corresponding steady-state buffer balance equations, while Eqs. 14 and 17 represent hydrogen-ion movement. Equation 14, for instance, says that the hydrogen ion "deposited" at the interface by conversion of RNH^+ to RN diffuses back to the mucosal bulk as H^+ or is carried there by conversion of B^- to BH, which diffuses back out to the bulk phase.

In addition, the following equilibria apply at all places in the aqueous phases:

$$KA = (RN)(H^+)/RNH^+ \quad \text{(Eq. 18)}$$

$$KB = (H^+)(B^-)/HB \quad \text{(Eq. 19)}$$

$$KC = (HC^-)(H^+)/H2C \quad \text{(Eq. 20)}$$

These are concentration dissociation constants as opposed to thermodynamic (activity) dissociation constants. They may be coupled with Eqs. 11–17 to give a system of seven equations in seven unknowns, G, B_1^-, HC_2^-, and the two interfacial concentrations of RN and H^+. This system of equations is then solved numerically by a digital computer program[3]. Inputs to this program include all pertinent bulk phase concentrations (buffer, drug, and hydrogen ion), dissociation constants of buffer and drug, barrier dimensions, diffusion coefficients, and the partition coefficient. Output consists of G and the concentrations of various species at the two aqueous–lipid interfaces. Results of sample calculations for a "physiological" system appear in Fig. 4 (14). The weak base is traveling between aqueous phases having pH's of 6.5 and 7.4. The data, shown as log–log plots, include the large range and domain of variables covered in the computations. As the pH-partition theory

[3] IBM 360/67 digital computer, University of Michigan Computing Center.

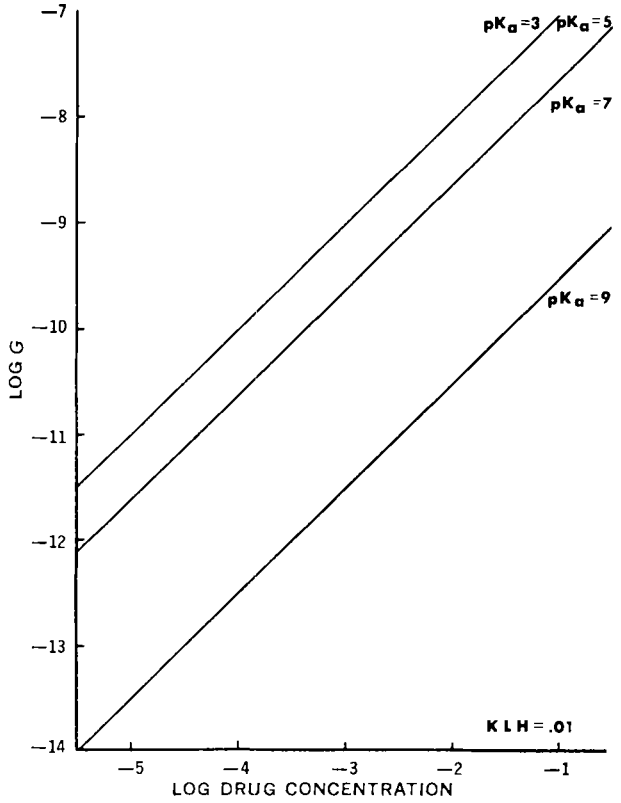

Figure 6—*Log* G versus *log intestinal concentration plots for amines of various pKa's and* KLH = 10^{-2}. *Intestinal pH = 6.5; blood pH = 7.4. Intestinal buffer concentration* = 1.0×10^{-2} M; *serum buffer concentration* = 2.6×10^{-2} M. *Serosal drug concentration* = 0.

would predict, the transport rate increases with the partition coefficient (other things being equal) in a 1:1 ratio. As observed in the calculations for neutral solutes, the leveling-off effect does occur at higher *KLH* values, when the aqueous diffusion layers make up the total barrier. The curve for the base with a pKa of 3 coincides with the curve in Fig. 2, indicating that the base is acting essentially as a nonelectrolyte at pH 6.5 in the mucosal phase. For weak bases of higher pKa values, the linear dependence of *G* on the partition coefficient is seen to extend over a somewhat wider range. This implies that the small fraction of uncharged species present at two or more pH units below the pKa makes the transport process dependent on the membrane permeability over a wider range of partition coefficient values. Transport rates of bases with higher pKa's are seen in Fig. 4 to level off at correspondingly lower values. Calculations with higher buffer strengths, however, give somewhat higher maximum rate plateaus for those bases having higher pKa values. For these pH conditions (serosal drug mainly in the uncharged form, RN), however, the plateaus cannot be made to approach those for lower pKa bases, even with infinite buffer strength.

Figure 5 shows concentration profiles, the results of computations based on equations similar to Eqs. 12–14 and 15–17. The boundary conditions were the interfacial concentrations of various species (obtained from computer calculation of the steady-state rate) and those at an arbitrary distance into the aqueous barriers. The aqueous concentration profiles are indeed curved, as predicted. The function of the buffers in hydrogen-ion movement is also evident.

Other computations (Figs. 6–8) have shown that the steady-state absorption rate is generally directly proportional to the overall concentration drop between the two bulk aqueous phases. Some limiting does occur in the case of high partition coefficient bases when the buffer concentration is not significantly greater than that of the base itself. Substitution of higher buffer concentrations linearizes the upper portions of the curves in Fig. 8. In any given experimental situation, it would be advisable to have a buffer concentration appreciably greater than that of the transporting solute.

Figure 9 summarizes the effect of the aqueous diffusion layer thickness on permeation rate. There is no, or relatively little, effect of aqueous barrier thickness on the movement of solutes having low

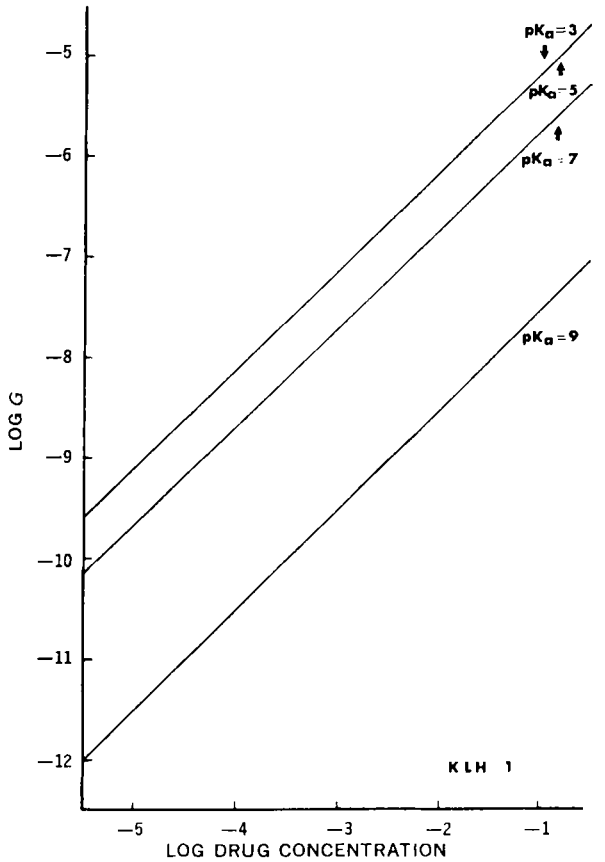

Figure 7—*Log* G versus ΔC *plots for amines of various pKa's and* KLH = *1. Note linearity of* G *with concentration difference across the membrane for these calculations, although* ΔC *may be greater than the buffer concentrations.*

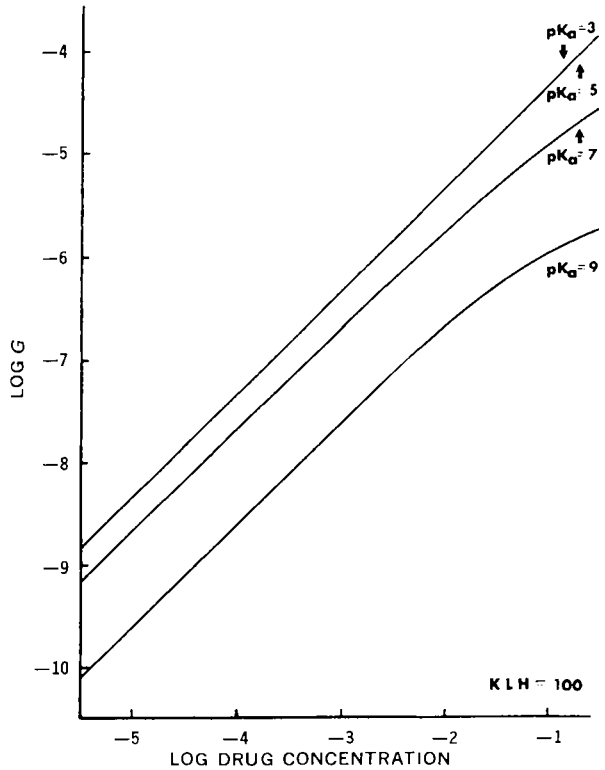

Figure 8—*Log* G versus *log* ΔC *plots for amines of various pKa's and* KLH = *100. Note deviations from linearity at higher amine concentrations for pKa = 7 and 9; buffer concentration is rate-limiting factor.*

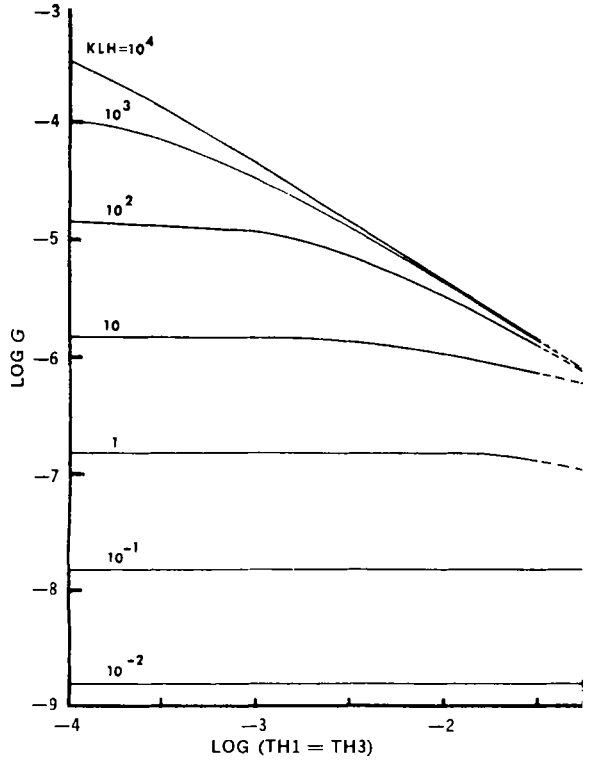

Figure 9—*Plot showing effect of the magnitude of aqueous barrier thickness (TH1 = TH3) on G for bases having various partition coefficients. pKa = 6; $D_W = 10^{-5}$; $D_L = 10^{-6}$; $\Delta C = 10^{-2}$ M; intestinal pH = 6.5; serosal pH = 8.0. Total buffer concentration in both aqueous phases = 10^{-1} M. TH2, the membrane thickness, = 5×10^{-2} cm.*

permeability coefficient values. At higher values, the membrane's contribution to the total barrier decreases, and a curvilinear dependence of G on TH1 = TH3 becomes apparent. Ultimately, G becomes inversely proportional to the magnitude of the aqueous barrier. Also visible in Fig. 9 is the leveling off of G with the increasing partition coefficient.

Significant is the fact that under certain pH conditions the serosal aqueous barrier may be effectively eliminated. The necessary conditions are: (*a*) the neutral form of the electrolyte has a high lipid permeability coefficient, (*b*) the mucosal phase has such a pH value that the electrolyte is mainly in the neutral form, and (*c*) the serosal phase has such a pH value that the electrolyte is mainly in the charged form.

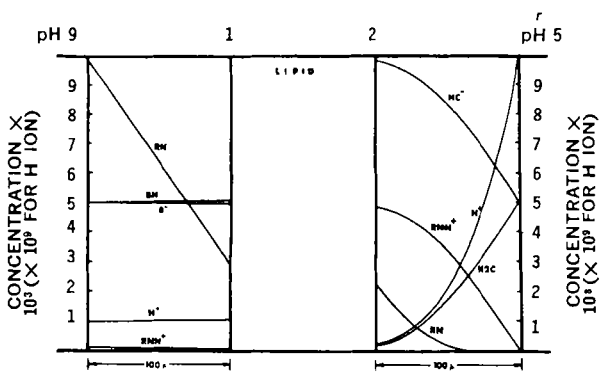

Figure 10—*Diagram showing concentration profiles in the two diffusion layers for the weak base of* KLH = *100 and pKa = 7, illustrating the special pH effect on rate. Total buffer concentration in either bulk phase = 10^{-2} M; pKa's of buffers are equivalent to respective bulk pH values. All diffusion coefficients = 10^{-5}. Mucosal base concentration = 10^{-2} M; serosal concentration = 0. Computer calculations give: G = 7.03×10^{-6} mmole cm.$^{-2}$ sec.$^{-1}$, $H_2^+ = 2.14 \times 10^{-7}$ M, $H_1^+ = 1.028 \times 10^{-9}$ M, $RN_2 = 2.238 \times 10^{-3}$ M, and $RN_1 = 2.941 \times 10^{-3}$ M, as well as buffer species concentrations at 1 and 2. These values plus equations similar to Eqs. 12–17 give illustrated profiles. The profile for RN in the lipid phase is off the scale of the diagram and is not shown.*

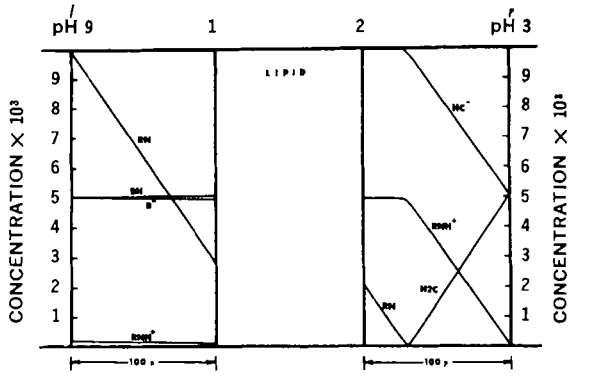

Figure 11—*Data obtained in a manner identical to Fig. 10. The serosal pH and pKa of the serosal buffer have been lowered to 3. Note that serosal RN drops to zero in even less distance than in Fig. 10. Note also the relatively small difference between RN values at the two oil–water interfaces.*

Figure 10 shows results of concentration profile calculations derived in a manner similar to those in Fig. 5. Note that the concentration of the uncharged form (RN) drops to zero in a distance from the serosal oil-water interface less than the entire diffusion layer thickness. This, in effect, increases the gradient for a given concentration drop. As a result, the overall concentration drop is increased to about 70% of the mucosal concentration. This figure should approach 100% as the partition coefficient is increased beyond 100.

Increasing the equilibrium constant for a reaction, such as RN + H2C $\rightleftarrows$ $RNH^+ + HC^-$, will, as predicted by Olander (15) for a simpler reacting system, result in more kinked concentration profiles. This is done in the present case by lowering the serosal pH and the pKa of the serosal buffer to, for example, 3, with the results shown in Fig. 11. The rate is virtually unchanged; the constant sum of the gradients of RN and RNH^+ is evident at various points.

Weak Acids—Figure 12 shows schematic gradients in the steady-state movement of an ionizing weak acid HR in the three-phase system. Equations 21–27 are entirely analogous to those (Eqs. 11–17) for the weak base:

$$G_{II} = (KLH)(D_{L,HR})(HR_1 - HR_2)/TH2 \quad \text{(Eq. 21)}$$

$$(TH1)(G_I) = D_{W,HR}(HR_1 - HR_1) + D_{W,R^-}(R_1^- - R_1^-) \quad \text{(Eq. 22)}$$

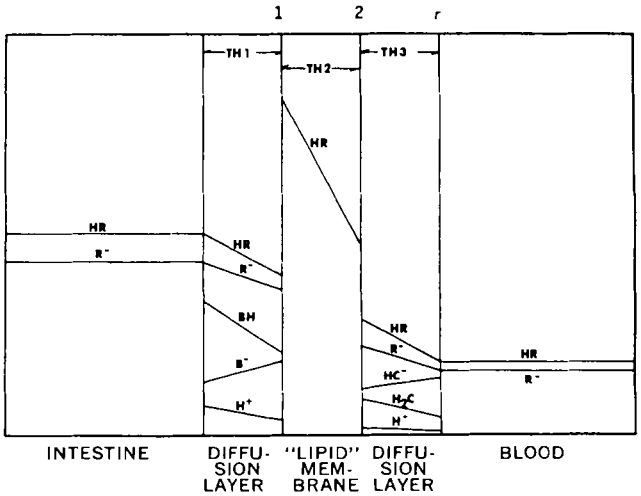

Figure 12—*Three-phase model showing schematic concentration profiles in steady-state transport of weakly acidic drugs, HR, which ionize to give R^-. Note movement of buffer species which supply or remove hydrogen ion at the interfaces.*

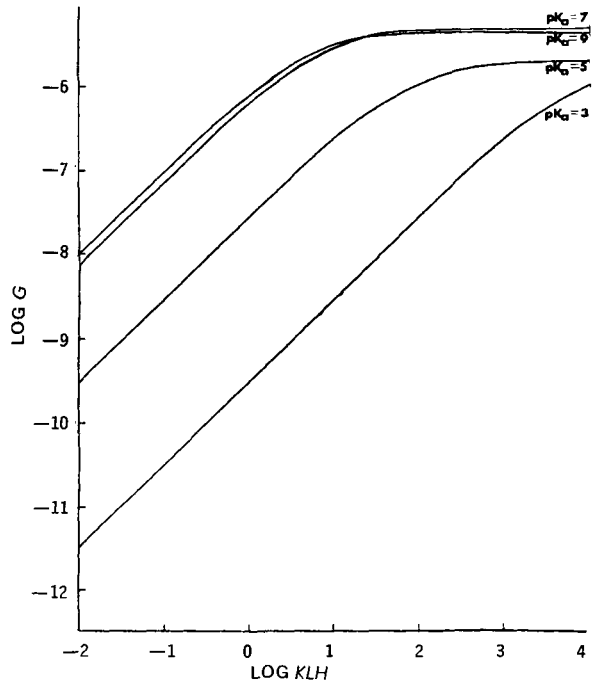

Figure 13—*Results of computations for the steady-state model for acid drugs, log* G versus *log* KLH. *All conditions are identical to those for weak bases (Fig. 4). Note anomalous behavior for pKa = 7 and pKa = 9 curves.*

$$-D_{W,B^-}(B_l^- - B_1^-) = D_{W,BH}(BH_l - BH_1) \quad \text{(Eq. 23)}$$

$$D_{W,H^+}(H_l^+ - H_1^+) + D_{W,BH}(BH_l - BH_1) = D_{W,R^-}(R_l^- - R_1^-) \quad \text{(Eq. 24)}$$

$$(TH3)(G_{III}) = D_{W,HR}(HR_2 - HR_r) + D_{W,R^-}(R_2^- - R_r^-) \quad \text{(Eq. 25)}$$

$$D_{W,HC^-}(HC_r^- - HC_2^-) = D_{W,H2C}(H2C_2 - H2C_r) \quad \text{(Eq. 26)}$$

$$D_{W,H2C}(H2C_2 - H2C_r) = D_{W,R^-}(R_2^- - R_r^-) + D_{W,H^+}(H_2^+ - H_r^+) \quad \text{(Eq. 27)}$$

These, along with the three dissociation constants for the buffers and the weak acid, are used to reduce the system to seven equations in seven unknowns.

Figure 13 shows results for computations using conditions identical to those used in Fig. 4 for the weak bases. Resulting transport rates are qualitatively as expected, with rates for acids of low pKa's, mostly dissociated at pH 6.5, being lower for any given partition coefficient value and reaching lower maximal rates than acids having higher pKa values. As before, however, the difference in plateaus decreases with higher buffer concentrations. Maximum rates for pKa 7 and 9 acids show the effects of the pH-dependent mechanism illustrated in Figs. 10 and 11; they are greater than the value (5.0×10^{-6} mmole cm.$^{-2}$ sec.$^{-1}$) expected for a strictly neutral solute. Figure 14 demonstrates the dependence of this effect on buffer concentration. Under optimum conditions (high partition coefficient and buffer strength), the expected rate-doubling occurs, reflecting the effective elimination of one-half of the total barrier.

It is apparent then that, given proper pH conditions, identical effects will be demonstrated by both acids and bases.

Transport of One Component when a Second Component Is Also Absorbed—In the GI tract, it is a known fact that only the distal portion of the small intestine is permeable to bile salts (16). A model has been constructed for the instance where the buffer has the capability of being absorbed. Figure 15 shows the case where the solute (PYR) and buffer (ETP) are both weak bases. The buffer is present in appreciably larger concentration than the solute itself. The original equations governing three-phase transport led to algebraic difficulties; hence a two-phase (aqueous–lipid) approximation was adopted. Here, the lipid phase essentially serves as a perfect sink. One can consider buffer and solute concentrations as dropping to zero at the right oil–water interface.

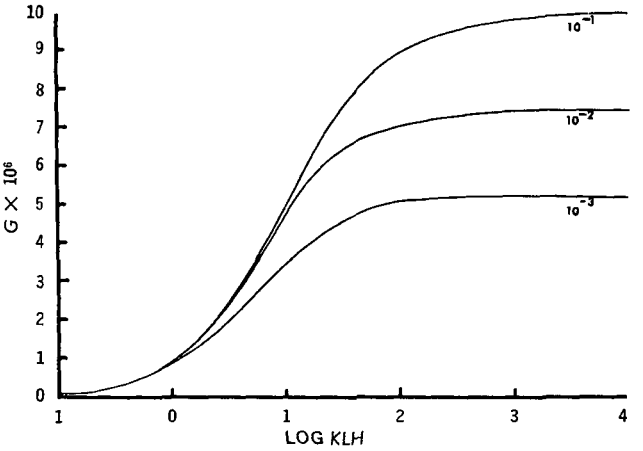

Figure 14—G versus *log* KLH *for a weak acid (pKa = 7) series at three different serosal–mucosal buffer concentrations. The maximum rate under these conditions for a strictly neutral solute is* 5×10^{-6} *mmole cm.*$^{-2}$ *sec.*$^{-1}$. *pH (intestine) = 5; pH (blood) = 9. TH1 = TH3 = 100 μ; TH2 =* 10^{-1} *cm. All diffusion coefficients =* 10^{-5} *cm.*^{2} *sec.*$^{-1}$. *Intestinal concentration of acid =* 10^{-2} M; *serosal bulk concentration = 0. For maximum buffer capacity, pKa's of buffers are equal to bulk pH values.*

The buffer is assumed to have an intrinsic partition coefficient significantly larger than that for the other solute.

The equations describing transport under these conditions appear below. PYR is the low partition coefficient solute; ETP is the buffer with a high partition coefficient. Subscripts *l* and 1 on various species refer to locations as previously defined. L and W on *G*'s and *D*'s refer to lipid and aqueous phases, respectively:

$$G_{PYR,L} = (KLH_{PYR})(D_{L,PYR})(PYR_1 - 0)/TH2 \quad \text{(Eq. 28)}$$

$$G_{ETP,L} = (KLH_{ETP})(D_{L,ETP})(ETP_1 - 0)/TH2 \quad \text{(Eq. 29)}$$

$$(TH1)(G_{ETP,W}) = D_{W,ETP}(ETP_l - ETP_1) + D_{W,ETPH^+}(ETPH_l^+ - ETPH_1^+) \quad \text{(Eq. 30)}$$

$$(TH1)(G_{PYR,W}) = D_{W,PYR}(PYR_l - PYR_1) + D_{W,PYRH^+}(PYRH_l^+ - PYRH_1^+) \quad \text{(Eq. 31)}$$

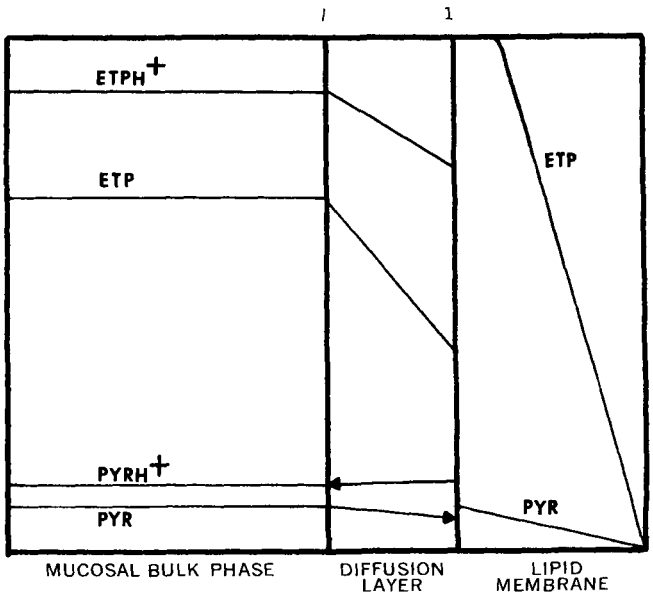

Figure 15—*Two-phase model (with a perfect sink) for transport of two basic solutes: a buffer, ETP, with a high partition coefficient, and another moiety, PYR, with a low partition coefficient. The deposition of* H^+ *at the interface from the conversion of* $ETPH^+$ *results in a lowering of interfacial pH.*

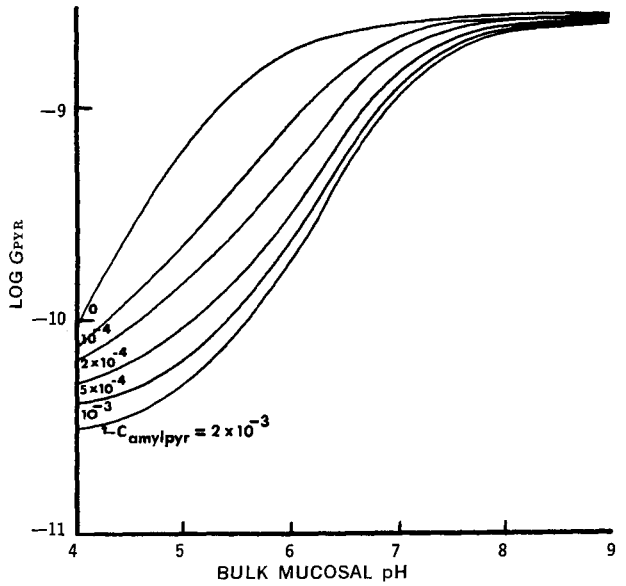

Figure 16—*Calculations showing the effect of transfer of a high partition coefficient weak base, AMYLPYR, on the rate of transfer of another base, PYR, having a relatively low partition coefficient. PYR = 10^{-4} M. Numbers on curves refer to aqueous bulk concentration of AMYLPYR.* D_W*'s =* 10^{-5}*;* D_L*'s =* 5×10^{-6}*. TH1 =* 2×10^{-2} *cm.; TH2, the membrane thickness, =* 5×10^{-2} *cm.* KLH *of AMYLPYR = 298;* KLH *of PYR = 0.275. The topmost curve, representing behavior in the absence of AMYLPYR, is essentially a normal titration curve for PYR.*

$$D_{W,ETPH^+}(ETPH_l^+ - ETPH_l^+) = D_{W,PYRH^+}(PYRH_l^+ - PYRH_l^+) + D_{W,H^+}(H_l^+ - H_l^+) \quad \text{(Eq. 32)}$$

Equations 28 and 29 are the steady-state transport expressions for the solute and buffer through the lipid phase. Equations 30 and 31 describe the movement of the two substances through the mucosal diffusion layer. Transport of hydrogen ion itself and by the two solutes is described by Eq. 32. These equations, along with dissociation constants of the two solutes, can be numerically solved to give the transport rates of the two bases as well as the interfacial concentrations of the various species in solution.

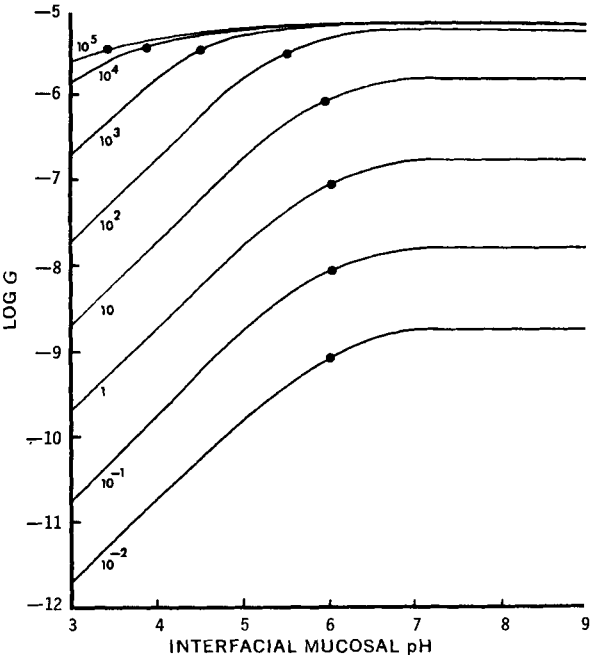

Figure 18—*Log of transport rate plotted against the interfacial mucosal pH values for conditions identical to those in Fig. 17, except serosal pH and pKa of buffer = 3. Numbers on curves are* KLH *values. Note apparent shift in profiles, as predicted by Suzuki* et al. *(11). Large dots indicate apparent pKa's.*

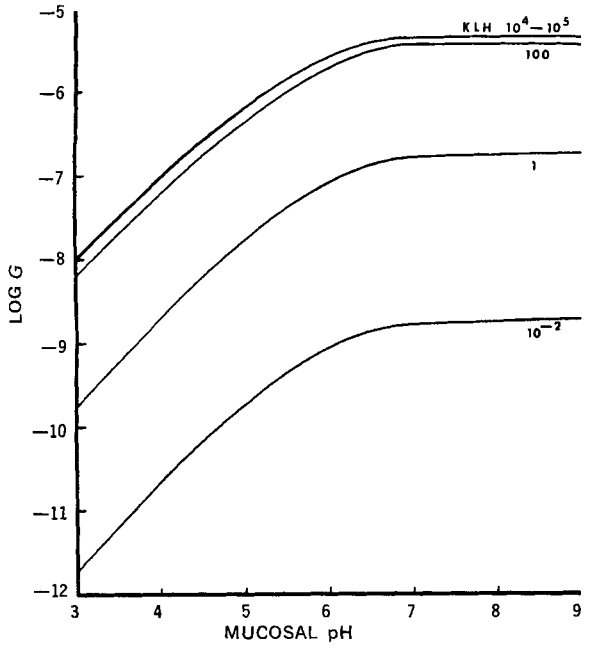

Figure 17—*pH–rate profiles in a three-phase system for weak bases of pKa = 6. Numbers on curves are partition coefficient values. Mucosal drug concentration =* 10^{-2} M; *buffer concentrations in both aqueous phases =* 10^{-2} M; *and serosal pH = 7.4. All aqueous diffusion coefficients =* 10^{-5}*;* $D_L = 10^{-6}$*. Buffer pKa's are equivalent to bulk pH values. TH1 = TH3 =* 10^{-2} *cm.; TH2 =* 5×10^{-2} *cm.* P = (D_L) (KLH)/*TH2 =* 2×10^{-6}·KLH*; therefore, the* T *value, the ratio of* D_W/*TH1*:P, = 50/KLH. *Note lack of shift under even extreme values of* KLH *(very low* T *values).*

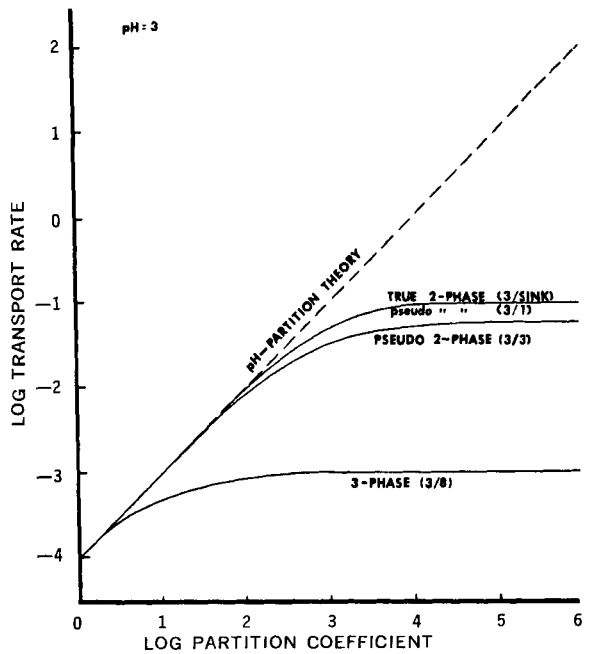

Figure 19—*Log transport rate* (G) versus *log partition coefficient* (KLH) *for a series of weak bases of pKa = 5 in a comparison of models when source phase pH = 3. Numbers in parentheses on curves refer to the pH of the source and receptor phases, respectively. The upper dashed line is the pH–partition theory prediction. Lowering receptor phase pH to 1 also gives results identical to the two-phase model. TH1 = TH2 = TH3 =* 10^{-2} *cm.;* $D_W = 10^{-5}$*;* $D_L = 10^{-6}$ *cm.*^{2} *sec.*$^{-1}$*; and* $\Delta C = 100$ *arbitrary concentration units.*

Figure 16 shows the effect of the transport of a basic buffer with a partition coefficient of 300 on the movement of another basic solute with a partition coefficient of less than one. At intermediate pH's, the rapid transport of the buffer affects the rate of the lower partition coefficient solute The interfacial pH, lower than the bulk pH, is the result of the outward gradient of H^+ apparent in Fig 15. H^+ is also carried out to the bulk by PYR as $PYRH^+$. Therefore, the net rate of PYR transport across the system is lowered. At higher mucosal pH values, however, where both bases are in the uncharged form, little or no effect is observed; both substances pass through the system independently of each other. The magnitude of the effect on the pH-rate profile of PYR, the lower partition coefficient solute, is dependent on the relative concentrations of solute and buffer.

Other similar models have been considered in a general way. An absorbable acid buffer can similarly inhibit the transport of an acid solute, while mixtures of an acid buffer and basic solute or a basic buffer and acid solute can result in mutual enhancement of transport rates.

Comparison to a Two-Phase Model—The two-phase model of Suzuki *et al.* (11, 12) for weak electrolytes led to a correlation between the relative resistances of the lipid (membrane) and aqueous (diffusion layer) phases and the shape of the pH–uptake rate constant profiles. Under conditions of high buffer strength, with the lipid acting as a perfect sink, the apparent pKa (defined as the interfacial pH where half the maximum rate constant is exhibited) is a function of T, the ratio of the permeability coefficient of the diffusion layer (D_W/TH1, as defined in the present terminology) to the permeability coefficient of the lipid phase [(KLH) (D_L)/TH2]. As T decreases (relative resistance of aqueous phase $\gg$ resistance of lipid phase), there is an apparent shift of the pH–rate profile toward lower pH values for weak bases and toward higher pH values for acids.

An appropriate serosal pH, low for bases and high for acids, allows the present three-phase model to simulate two-phase conditions. If this is not done, normal three-phase conditions prevail, resulting in the profiles of Fig. 17. Lowering the serosal pH results in Fig. 18, with a pronounced leftward shift in the pH–rate profiles with increasing partition coefficient. It is also apparent that with a high buffer concentration and diffusivity, there should be no visible variation of G with mucosal pH.

DISCUSSION

Hogben *et al.* (2) noted the possible importance of drug diffusion to the intestinal mucosa under favorable absorption conditions. The nondependence of the transport rate on the partition coefficient

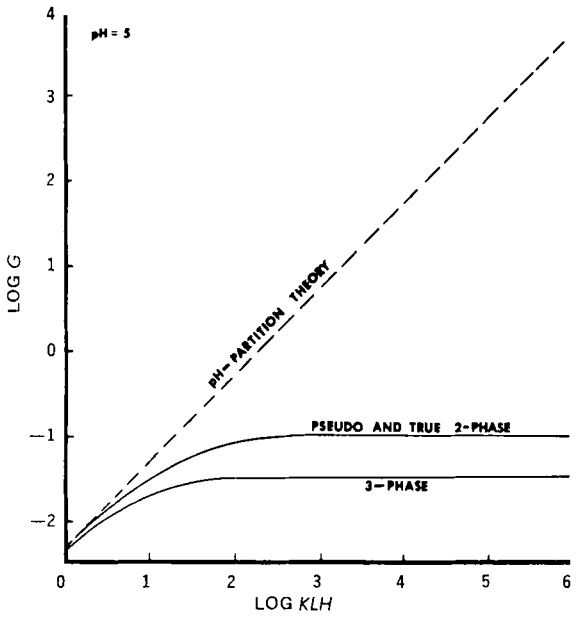

Figure 20—*Log* G versus *log* KLH *for a series of weak bases, pKa = 5, when source phase pH = 5. Other conditions are as for Fig. 19.*

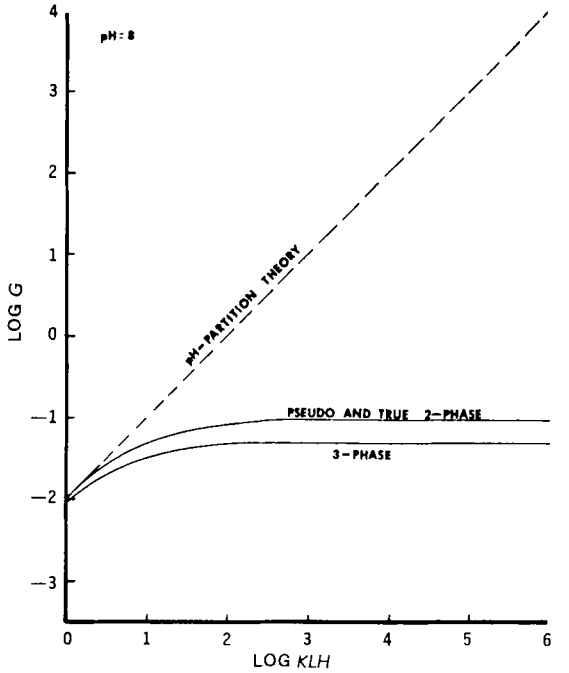

Figure 21—*Log* G versus *log* KLH *for a series of weak bases, pKa = 5, when source phase pH = 8. Other conditions are as for Fig. 19.*

when the latter is high was utilized in the work of Howard *et al.* (10).

The present model enables a fresh interpretation of studies in the literature. Koizumi *et al.* (17) noted an increased absorption constant with a greater rate of recirculation of drug solution through the rat intestine, possibly resulting from a decreased aqueous diffusion barrier. The data of Misra *et al.* (18), for transport of salicylic acid through collodion membranes, indicate that these barriers must be permeable to salicylate ion. The permeation rate from a compartment of pH 3 was only about eight times that from a compartment of pH 8.5. The difference in the relative percent of acid in the neutral form would be about five orders of magnitude between the two pH's, and considerations in the viewpoint of the present model would require rather drastic conditions.

The lack of physicochemical definition of three-phase *in vitro* systems often makes impossible the evaluation of the aqueous diffusion barriers' contribution. The studies of Garrett and Chemburkar (19, 20) and of Levy and Mroszczak (21) illustrate classical membrane-limited transport rates. The movement of salicylic acid through an olive oil-saturated Millipore filter disk in the latter study could, however, depend somewhat on the aqueous portion of the total barrier. The lack of stirring in the aqueous chambers between samples precludes accurate interpretation.

The buccal absorption data of Beckett and Moffat (22) indicate, for high partition coefficient solutes, a dependence on diffusion through an aqueous barrier adjacent to the buccal mucosa. This was confirmed by recent model studies (23).

In a study of the movement of a series of carboxylic acids across the toad bladder membrane (24), several interesting points were made. Calculated permeability constants for nonionic species apparently leveled off above the six-carbon acid. In this three-phase system, the receptor aqueous phase was at pH 7, creating an effective two-phase system and eliminating the serosal diffusion layer. Highly lipid-soluble acids would exhibit a shift in the mucosal pH–transport rate profiles toward a higher pH. The rate for a mucosal pH of 6 would, therefore, be expected to be the same or very little less than that for pH 4–5. This was borne out in the experimental results. Moreover, it is possible that the buffer in the system was of sufficient concentration and capacity to decrease further the expected rate difference between pH 4 and 6 by facilitating the conversion of the anion of the acid to the uncharged form. The authors, however, attributed the behavior to a direct pH effect on the membrane itself; *i.e.*, the membrane was more permeable to the free acid at pH 6 than at pH 4. More importantly, they stated that "highly lipid soluble acids may reach a limiting penetration rate."

While the models discussed in the present research may not generally explain the complex *in vivo* absorption of drugs, they should contribute significantly to the understanding of baseline behaviors. They, therefore, provide at least a systematic understanding of the simultaneous interaction of the many physicochemical variables in the system, leading often to unexpected results. As future work should show, these models and their elaboration to handle more complex situations should prove very valuable in both experimental design and data analysis of *in vivo* studies.

ADDENDA

It would be instructive to compare the various models (two phase, pseudo two phase, and three phase) under identical source phase pH conditions to answer the following question: How closely, and under what conditions, does the pseudo-two-phase model approximate the true two-phase model (11, 12) where the lipid phase acts as a perfect sink?

Figures 19–21 compare the three models for a homologous series of bases with a pKa of 5 when the pH of the source phase is 3, 5, and 8, respectively. A simplifying assumption in these calculations is very large buffer strength; hence, interfacial pH is equivalent to bulk pH. In all three figures, it is apparent that all models (and the pH-partition theory prediction, based on concentration of the unionized species in the source phase and no aqueous diffusion layers) are equivalent for low partition coefficient solutes. The membrane is overwhelmingly the rate-determining barrier. As the partition coefficient increases, however, the three *diffusional* models show the leveling-off trend. The true three-phase model in Fig. 19 (3/8) levels off at a rate 1% of the true two-phase model value. It is also seen that the pseudo-two-phase model (3/3) does not approximate the true two-phase model (3/sink). When the fraction of base as RN in the source phase increases to 50 and 100% (Figs. 20 and 21), however, the models do converge.

At first glance, then, it would appear that the three-phase model can, in the form of the pseudo-two-phase model, be made to approximate true two-phase conditions whenever an appreciable amount of the solute is in the uncharged form in the source phase and is mainly in the charged form in the receptor phase. However, as the upper solid curve in Fig. 19 indicates, lowering the receptor phase pH from 3 to 1 again equalizes the pseudo- and true two-phase models. It may thus be summarized that the pseudo-two-phase model accurately simulates two-phase conditions simply when there is proportionately more uncharged solute in the source phase than in the receptor phase. This is in concurrence with the results of Ho and Higuchi (23) for buccal absorption of weak acids. Since salivary pH (6.0–7.0) is less than serosal pH (7.4), there is proportionately more uncharged acid in the oral solution; hence, the two-phase model does apply. As stated by Ho and Higuchi (23), this would not be the case for buccal absorption of weak bases.

REFERENCES

(1) L. S. Schanker, D. J. Tocco, B. B. Brodie, and C. A. M. Hogben, *J. Pharmacol. Exp. Ther.*, **123,** 81(1958).

(2) C. A. M. Hogben, D. J. Tocco, B. B. Brodie, and L. S. Schanker, *ibid.*, **125,** 275(1959).

(3) P. A. Shore, B. B. Brodie, and C. A. M. Hogben, *ibid.*, **119,** 361(1957).

(4) L. S. Schanker, P. A. Shore, B. B. Brodie, and C. A. M. Hogben, *ibid.*, **120,** 528(1957).

(5) C. A. M. Hogben, L. S. Schanker, D. J. Tocco, and B. B. Brodie, *ibid.*, **120,** 540(1957).

(6) J. T. Doluisio and J. V. Swintosky, *J. Pharm. Sci.*, **53,** 597 (1964).

(7) J. Perrin, *ibid.*, **56,** 411(1967).

(8) M. A. Augustine and J. Swarbrick, *ibid.*, **59,** 314(1970).

(9) S. A. Howard, M. A. Farvar, A. Suzuki, and W. I. Higuchi, *ibid.*, **58,** 1325(1969).

(10) *Ibid.*, **58,** 1330(1969).

(11) A. Suzuki, W. I. Higuchi, and N. F. H. Ho, *J. Pharm. Sci.*, **59,** 644(1970).

(12) *Ibid.*, **59,** 651(1970).

(13) H. Passow, *J. Theor. Biol.*, **17,** 383(1967).

(14) R. G. Stehle and W. I. Higuchi, *J. Pharm. Sci.*, **56,** 1367 (1967).

(15) D. R. Olander, *AIChE J.*, **6,** 233(1960).

(16) J. R. Senior, *J. Lipid Res.*, **5,** 495(1964).

(17) T. Koizumi, T. Arita, and K. Kakemi, *Chem. Pharm. Bull.*, **12,** 421(1964).

(18) A. L. Misra, A. Hunger, and H. Keberle, *J. Pharm. Pharmacol.*, **18,** 531(1966).

(19) E. R. Garrett and P. B. Chemburkar, *J. Pharm. Sci.*, **57,** 944 (1968).

(20) *Ibid.*, **57,** 949(1968).

(21) G. Levy and E. J. Mroszczak, *J. Pharm. Sci.*, **57,** 235(1968).

(22) A. H. Beckett and A. C. Moffat, *J. Pharm. Pharmacol.*, **20,** 239S(1968).

(23) N. F. H. Ho and W. I. Higuchi, *J. Pharm. Sci.*, **60,** 537 (1971).

(24) H. Rosen, A. Leaf, and W. B. Schwartz, *J. Gen. Physiol.*, **48,** 379(1964).

(25) P. Singh, S. J. Desai, D. R. Flanagan, A. P. Simonelli, and W. I. Higuchi, *J. Pharm. Sci.*, **57,** 959(1968).

ACKNOWLEDGMENTS AND ADDRESSES

Received June 4, 1971, from the *College of Pharmacy, University of Michigan, Ann Arbor, MI 48104*

Accepted for publication July 12, 1972.

Presented to the Basic Pharmaceutics Section, APhA Academy of Pharmaceutical Sciences, Washington, D. C. meeting, April 1970.

Abstracted from a thesis submitted by R. G. Stehle to the University of Michigan in partial fulfillment of the Doctor of Philosophy degree requirements.

Supported by Grant GM-13368 and Predoctoral Fellowship 1-F1-GM-30,048-05 from the National Institute of General Medical Sciences, U. S. Public Health Service, Bethesda, MD 20014

* Present address: The Upjohn Co., Kalamazoo, MI 49001

▲ To whom inquiries should be directed.